**Supporting Information for**

# Vulnerability to APOBEC3G linked to the pathogenicity of deltaretroviruses.

Takafumi Shichijo[1, 2], Jun-ichirou Yasunaga[1, 2, *], Kei Sato[3, 4], Kisato Nosaka[1], Kosuke Toyoda[1, 2], Miho Watanabe[1], Wenyi Zhang[1], Yoshio Koyanagi[5], Edward L. Murphy[6, 7], Roberta L. Bruhn[7], Ki-Ryang Koh[8], Hirofumi Akari[9], Terumasa Ikeda[10, 11, 12], Reuben S. Harris[11, 12], Patrick L. Green[13], and Masao Matsuoka[1, 2, *]

**Corresponding Authors:**
Masao Matsuoka, Jun-ichirou Yasunaga
Email: mamatsu@kumamoto-u.ac.jp, jyasunag@kumamoto-u.ac.jp

**This PDF file includes:**
Figures S1 to S10
Tables S1 to S2

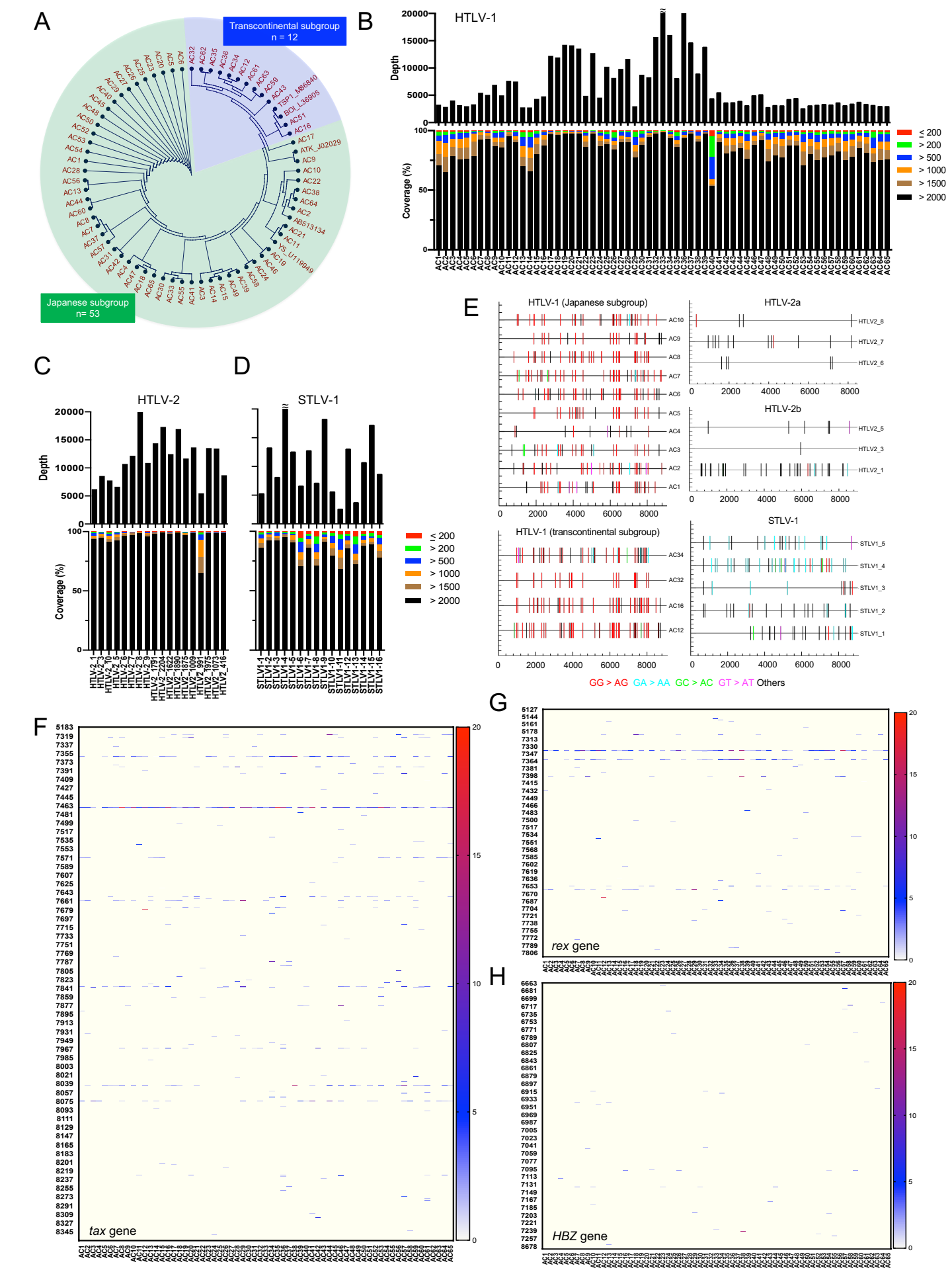
A
Transcontinental subgroup
n = 12
Japanese subgroup
n= 53
B
HTLV-1
Depth
Coverage (%)
≤ 200
> 200
> 500
> 1000
> 1500
> 2000
C
HTLV-2
D
STLV-1
E
HTLV-1 (Japanese subgroup)
HTLV-1 (transcontinental subgroup)
HTLV-2a
HTLV-2b
STLV-1
GG > AG GA > AA GC > AC GT > AT Others
F
tax gene
G
rex gene
H
HBZ gene

**Fig. S1. Deep sequencing of HTLV-1, HTLV-2, and STLV-1 proviruses *in vivo*.**
(*A*) Circular cladogram showing the HTLV-1 subgroups (green, Japanese subgroup [n = 53]; blue, transcontinental subgroup [n = 12]). References strains are indicated in the tree: ATK_J02029, YS_U119949, and AB513134 are Japanese subgroup; TSP1_M86840 and BOI_L36905 are transcontinental subgroup. (*B-D*) Depth (top) and the percentage of targeted bases covered by ≤ 200 ×, > 200 ×, > 500 ×, > 1000 ×, > 1500 × and > 2000 × sequencing reads (bottom) from deep sequencing analysis of the provirus in HTLV-1 asymptomatic carriers (ACs) (n = 65) (*B*), HTLV-2-infected individuals (n = 18) (*C*), and STLV-1-infected Japanese macaques (n = 16) (*D*). (*E*) Example of mutations in HTLV-1 asymptomatic carriers (ACs; Japanese subgroup, n = 10; transcontinental subgroup, n = 4), HTLV-2-infected individuals (HTLV-2a, n = 3; HTLV-2b, n = 3), and STLV-1-infected Japanese macaques (n = 5), analyzed by HYPERMUT(https://www.hiv.lanl.gov/content/sequence/HYPERMUT/hypermut.html). Reference sequences were AB513134 for HTLV-1 Japanese subgroup, L36905 for HTLV-1 transcontinental subgroup, NC_001488 for HTLV-2a, L20734 for HTLV-2b and MH542226 for STLV-1. (*F-H*) Heatmaps of mutations observed in the *tax* gene (*F*), *rex* gene (*G*), and *HBZ* gene (*H*) in 65 HTLV-1 ACs.

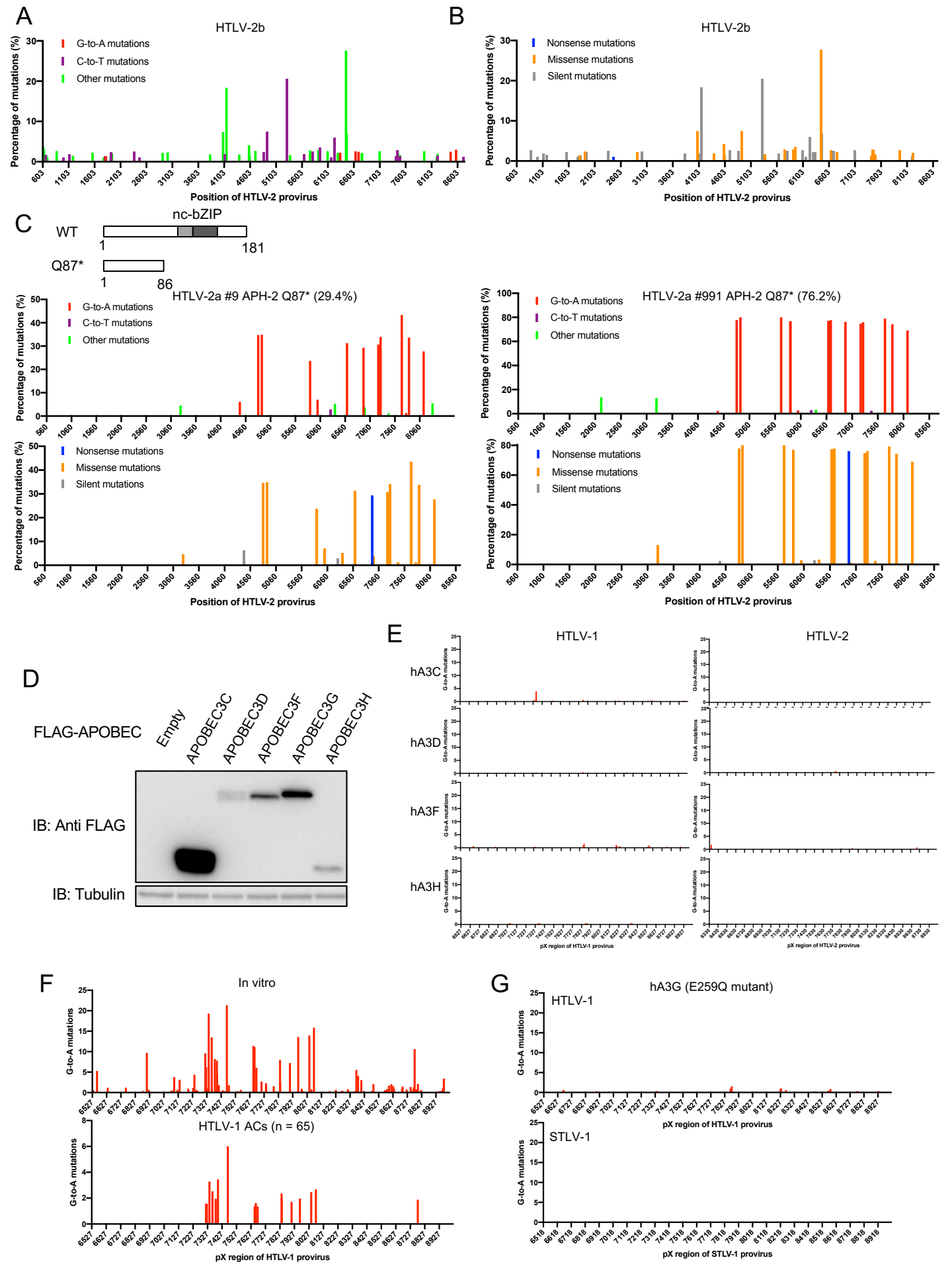
A
HTLV-2b
G-to-A mutations
C-to-T mutations
Other mutations
Percentage of mutations (%)
Position of HTLV-2 provirus
B
HTLV-2b
Nonsense mutations
Missense mutations
Silent mutations
Percentage of mutations (%)
Position of HTLV-2 provirus
C
nc-bZIP
WT
1
181
Q87*
1
86
HTLV-2a #9 APH-2 Q87* (29.4%)
G-to-A mutations
C-to-T mutations
Other mutations
Nonsense mutations
Missense mutations
Silent mutations
Percentage of mutations (%)
Position of HTLV-2 provirus
HTLV-2a #991 APH-2 Q87* (76.2%)
G-to-A mutations
C-to-T mutations
Other mutations
Nonsense mutations
Missense mutations
Silent mutations
Percentage of mutations (%)
Position of HTLV-2 provirus
D
FLAG-APOBEC
Empty
APOBEC3C
APOBEC3D
APOBEC3F
APOBEC3G
APOBEC3H
IB: Anti FLAG
IB: Tubulin
E
HTLV-1
HTLV-2
hA3C
hA3D
hA3F
hA3H
G-to-A mutations
pX region of HTLV-1 provirus
pX region of HTLV-2 provirus
F
In vitro
G-to-A mutations
HTLV-1 ACs (n = 65)
G-to-A mutations
pX region of HTLV-1 provirus
G
hA3G (E259Q mutant)
HTLV-1
G-to-A mutations
pX region of HTLV-1 provirus
STLV-1
G-to-A mutations
pX region of STLV-1 provirus

**Fig. S2. Deep sequencing of HTLV-1, HTLV-2, and STLV-1.**
(*A*) Frequency of mutations detected in the provirus of five HTLV-2b-infected individuals by deep sequencing analysis. (*B*) Frequency of nonsense mutations detected in the provirus of five HTLV-2b-infected individuals by deep sequencing analysis. (*C*) Schema of wild-type and mutants with a nonsense mutation (Q87*) in the *APH-2* gene in two cases (#9 and #991). Frequencies of provirus mutations in these two HTLV-2-infected individuals (#9 and #991): (top) G-to-A mutations and (bottom) nonsense mutations. (*D*) Immunoblot showing the expression of APOBEC families in transfected HEK293T cells. IB, immunoblot. (*E*) Frequency of mutations detected in the provirus of HTLV-1-infected cells (left) or HTLV-2-infected cells (right) with hA3C/D/F/H expression *in vitro*. (*F*) Frequency of mutations detected in HTLV-1-infected cells under hA3G expression *in vitro* (top) corresponds with that in more than 10% of HTLV-1 ACs (n=65) *in vivo* (bottom). (*G*) Frequency of mutations detected in HTLV-1-infected cells (top) and STLV-1-infected cells (bottom) under E259Q mutant hA3G expression *in vitro.*

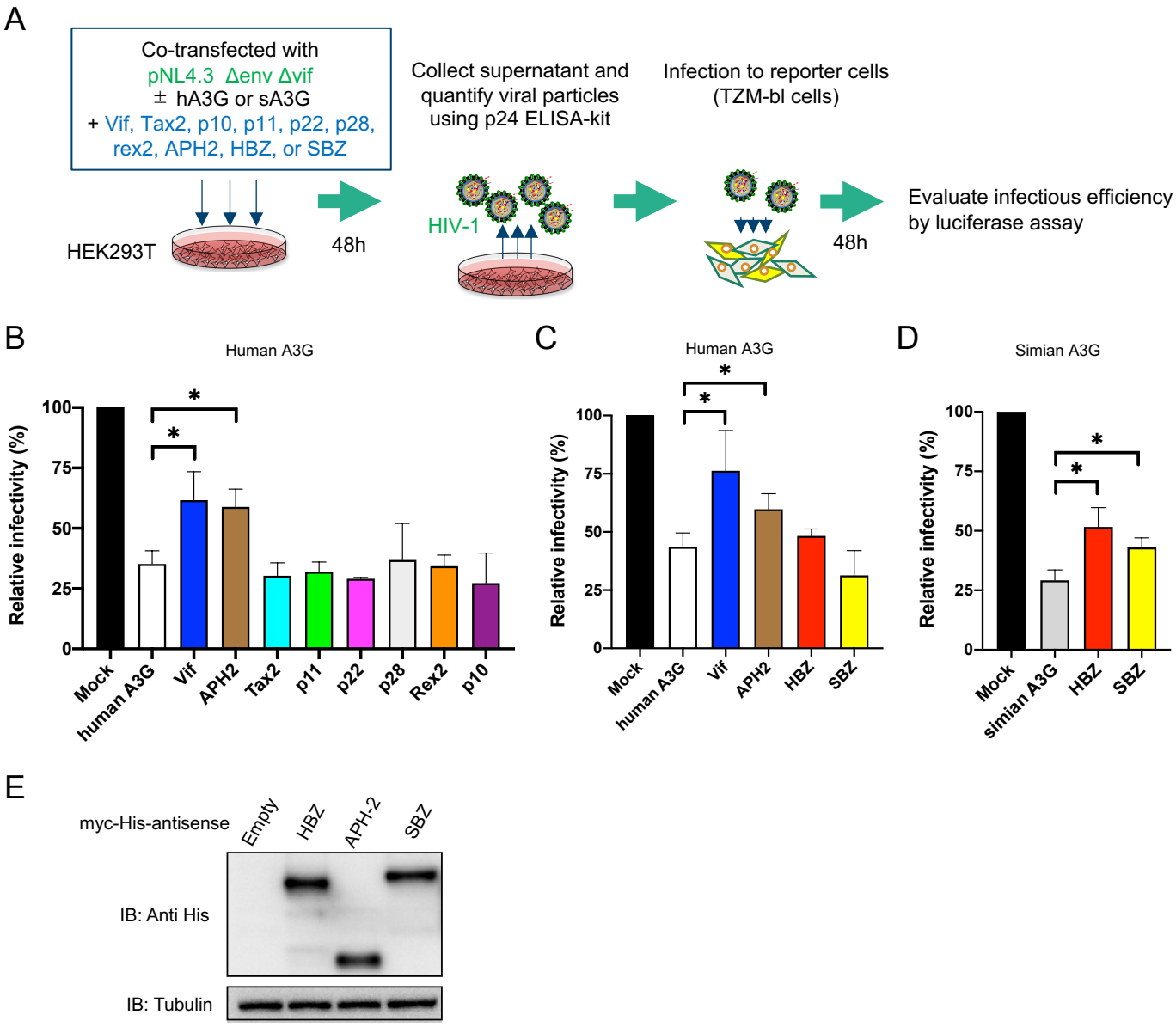


**Fig. S3. Antisense proteins suppress A3G.**

(*A*) Schema of the experiment to analyze the effects of HTLV-2 encoded genes and antisense viral proteins on viral infectivity in the presence of A3G using TZM-bl cells. Pseudotype recombinant HIV-1 (pNL4.3/ΔVif/ΔEnv) is produced using 293T cells expressing A3G and various viral genes. Vif is used as a positive control. (*B*) Among all the HTLV-2 coding proteins tested, only APH2 restored viral infectivity in the presence of hA3G (normalized mean ± s.d. of triplicate experiments; two-tailed unpaired Student's t test; *P < 0.05). (*C*) Of the antisense proteins of HTLV-2, HTLV-1, or STLV-1, APH2 best inhibits human A3G and restores infectivity (normalized mean ± s.d. of triplicate experiments; two-tailed unpaired Student's t test; *P < 0.05). (*D*) The antisense proteins of HTLV-1 or STLV-1 can inhibit simian A3G and restore infectivity (normalized mean ± s.d. of triplicate experiments; two-tailed unpaired Student's t test; *P < 0.05). (*E*) Immunoblotting showing the antisense proteins purified from QT6 cells overexpressing HBZ, APH-2, or SBZ. All experiments were performed at least twice.

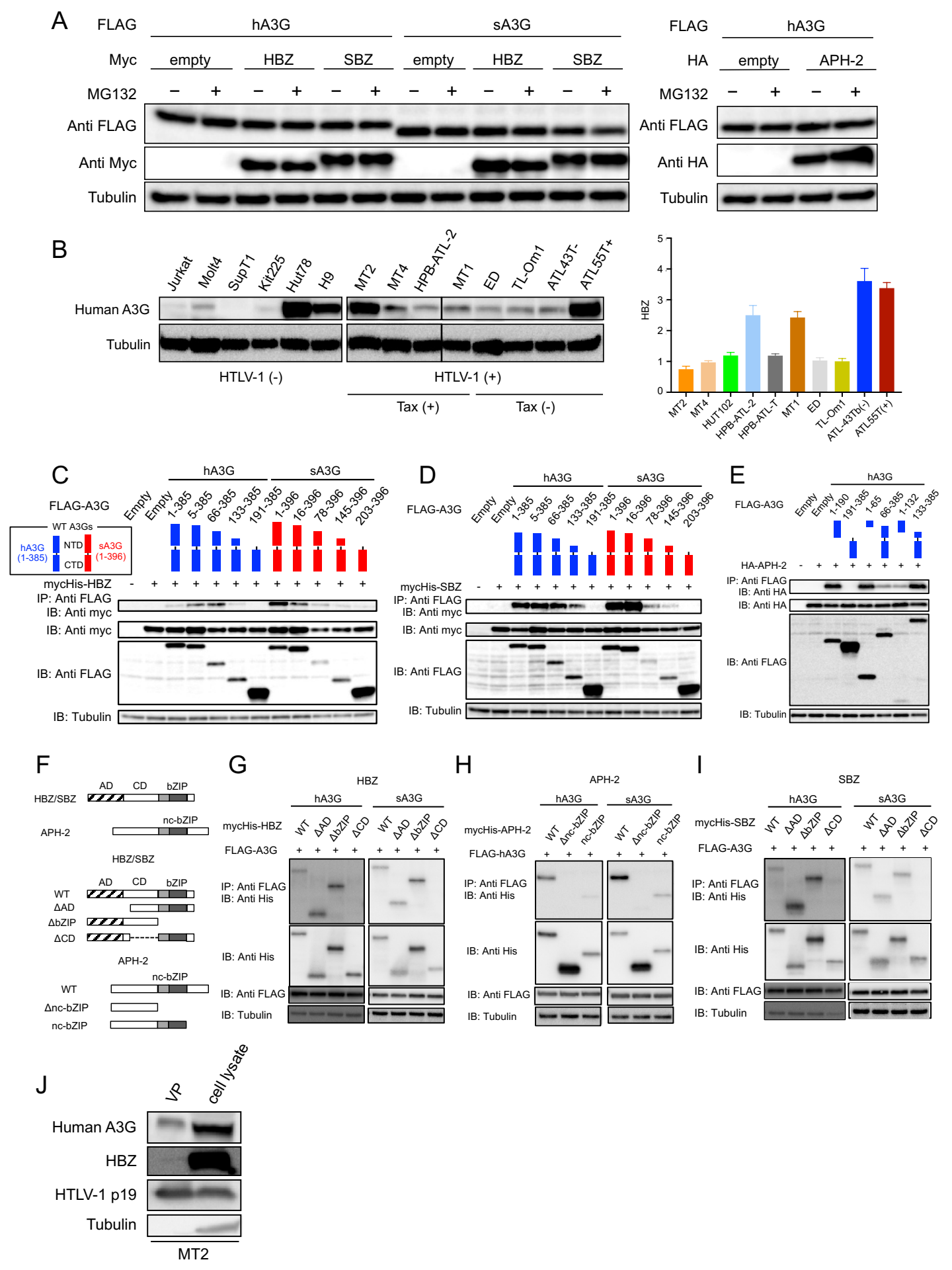
A
FLAG
hA3G
sA3G
Myc
empty
HBZ
SBZ
MG132
Anti FLAG
Anti Myc
Tubulin
FLAG
hA3G
HA
empty
APH-2
Anti HA
B
Jurkat
Molt4
SupT1
Kit225
Hut78
H9
MT2
MT4
HPB-ATL-2
MT1
ED
TL-Om1
ATL43T-
ATL55T+
Human A3G
HTLV-1 (-)
HTLV-1 (+)
Tax (+)
Tax (-)
HBZ
HUT102
HPB-ATL-T
ATL-43Tb(-)
C
FLAG-A3G
WT A3Gs
hA3G (1-385)
NTD
CTD
sA3G (1-396)
Empty
1-385
5-385
66-385
133-385
191-385
1-396
16-396
78-396
145-396
203-396
mycHis-HBZ
IP: Anti FLAG
IB: Anti myc
IB: Anti FLAG
IB: Tubulin
D
mycHis-SBZ
E
HA-APH-2
1-190
191-385
1-65
66-385
1-132
133-385
IB: Anti HA
F
AD
CD
bZIP
HBZ/SBZ
APH-2
nc-bZIP
WT
ΔAD
ΔbZIP
ΔCD
Δnc-bZIP
G
HBZ
mycHis-HBZ
FLAG-A3G
IP: Anti FLAG
IB: Anti His
H
APH-2
mycHis-APH-2
FLAG-hA3G
I
SBZ
mycHis-SBZ
J
VP
cell lysate
Human A3G
HBZ
HTLV-1 p19
Tubulin
MT2

**Fig. S4. Interaction between A3G and antisense viral proteins.**
(*A*) Immunoblot showing that the amount of A3G is unchanged in the presence or absence of antisense proteins with or without MG132 treatment. (*B*) Immunoblot showing the expression of endogenous hA3G in HTLV-1-negative T-cell lines (Jurkat, Molt4, SupT1, Kit225, Hut78, and H9), HTLV-1-infected T-cell lines (MT-2, and MT-4), and ATL cell lines (HPB-ATL-2, MT-1, ED, TL-Om1, ATL43Tb(-), and ATL55T+)(left). Expression of mRNA of *HBZ* in HTLV-1-infected T-cell lines (MT-2, MT-4, and Hut102), and ATL cell lines (HPB-ATL-2, HPB-ATL-T, MT-1, ED, TL- Om1, ATL43Tb(-), and ATL55T(+)) by RT-qPCR (right). (*C*-*E*) Co-immunoprecipitation experiments showing the interaction of deletion mutants of A3Gs with HBZ (*C*), SBZ (*D*) and APH-2 (*E*) in transfected HEK293T cells. IP, immunoprecipitation; IB, immunoblot. (*F*) Schema of wild-type and deletion mutants of HBZ/SBZ and APH-2. (*G*-*I*) Co-immunoprecipitation experiment showing the interaction of A3Gs with deletion mutants of HBZ (*G*), APH-2 (*H*) and SBZ (*I*) in transfected HEK293T cells. IP, immunoprecipitation; IB, immunoblot. (*J*) Immunoblot showing the incorporation of both hA3G and HBZ into viral particles in MT-2 cells. Experiments were performed at least twice.

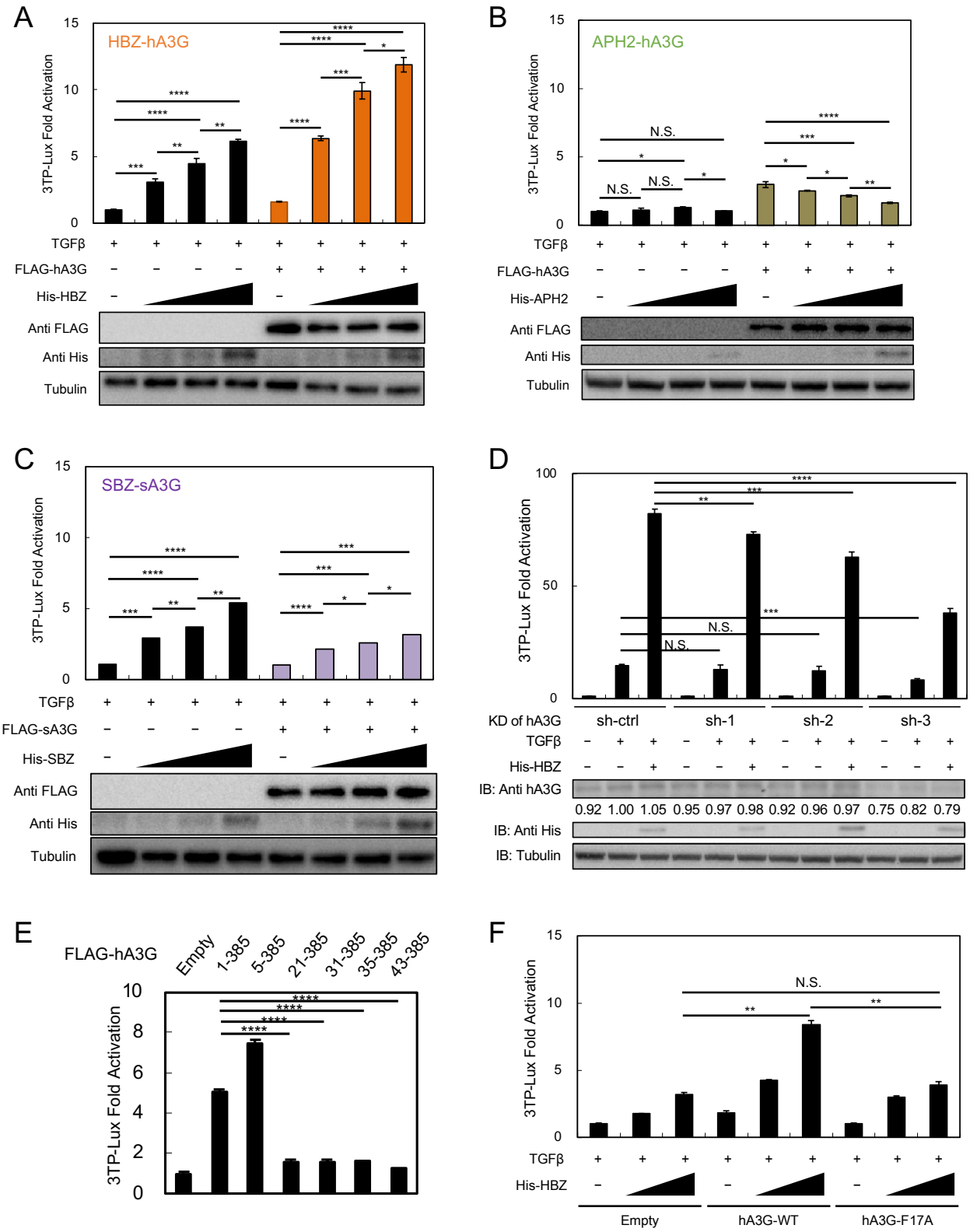
A
HBZ-hA3G
3TP-Lux Fold Activation
TGFβ
FLAG-hA3G
His-HBZ
Anti FLAG
Anti His
Tubulin
B
APH2-hA3G
N.S.
His-APH2
C
SBZ-sA3G
FLAG-sA3G
His-SBZ
D
KD of hA3G
sh-ctrl
sh-1
sh-2
sh-3
IB: Anti hA3G
0.92 1.00 1.05 0.95 0.97 0.98 0.92 0.96 0.97 0.75 0.82 0.79
IB: Anti His
IB: Tubulin
E
FLAG-hA3G
Empty
1-385
5-385
21-385
31-385
35-385
43-385
F
His-HBZ
Empty
hA3G-WT
hA3G-F17A

**Fig. S5. hA3G enhances the activation of the TGF-β/Smad pathway by HBZ.**
(*A*-*C*) Luciferase activity of 3TP-Lux under the control of a TGF-β responsive element in cells co-expressing hA3G with HBZ (*A*), hA3G with APH-2 (*B*), or sA3G with SBZ (*C*) (normalized mean ± s.d. of triplicate experiments; two-tailed unpaired Student's t test; *P < 0.05; **P < 0.01; ***P < 0.001; **** P < 0.0001). (*D*) Luciferase activity of 3TP-Lux under the control of a TGF-β responsive element in hA3G knockdown HepG2 cells expressing HBZ (normalized mean ± s.d. of triplicate experiments; two-tailed unpaired Student's t test; **P < 0.01; ***P < 0.001; **** P < 0.0001). The hA3G expression values were analyzed by ImageJ. (*E*) Luciferase activity of 3TP-Lux under the control of a TGF-β responsive element in cells expressing deletion mutants of hA3G (normalized mean ± s.d. of triplicate experiments; two-tailed unpaired Student's t test; **** P < 0.0001). (*F*) Luciferase activity of 3TP-Lux under the control of a TGF-β responsive element in cells co-expressing HBZ with empty, hA3G-WT, or hA3G-F17A mutant (normalized mean ± s.d. of triplicate experiments; two-tailed unpaired Student's t test; **P < 0.01). All experiments were performed at least twice.

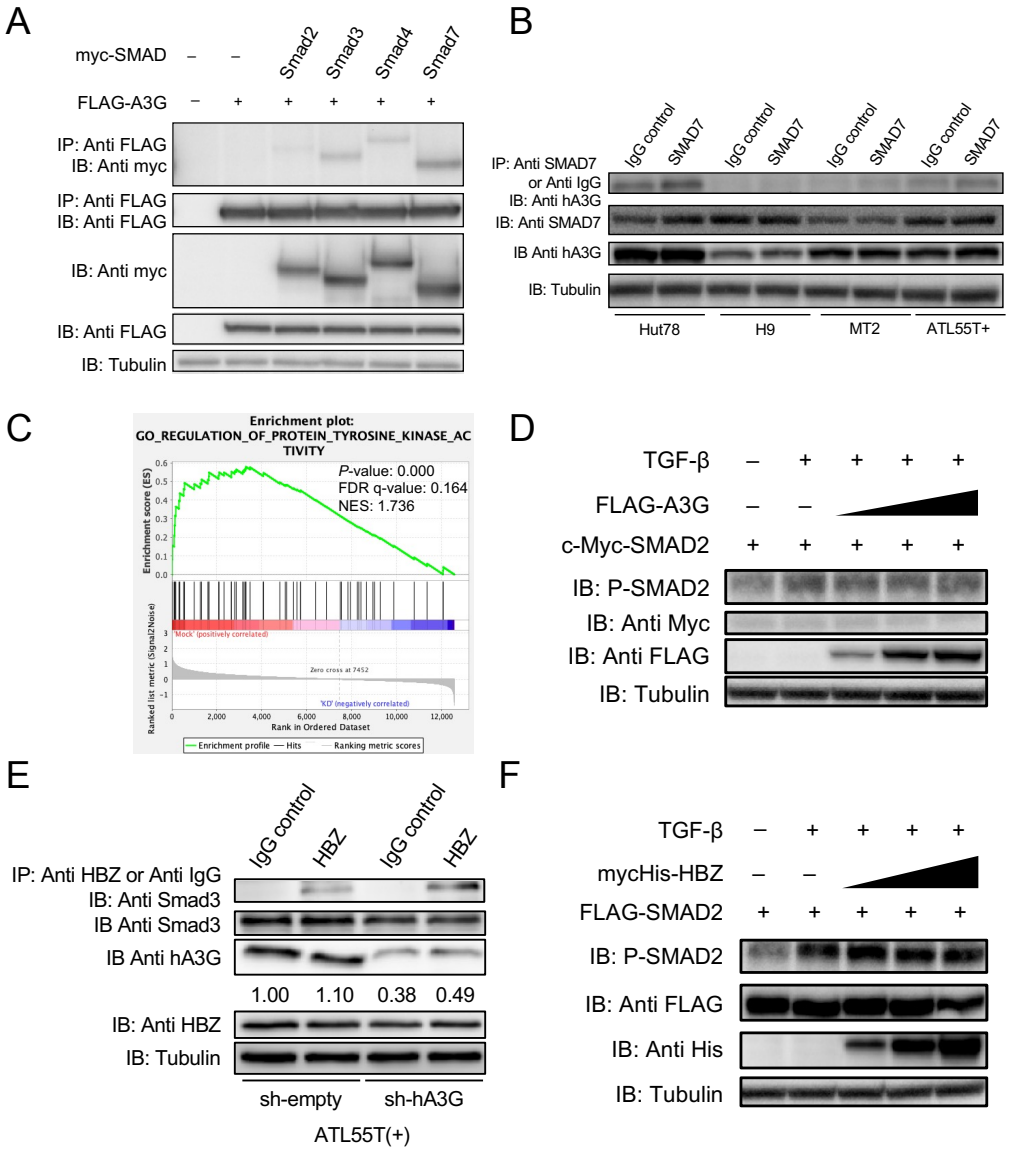


**Fig. S6. Interaction of hA3G with Smad proteins.**

(*A*) Co-immunoprecipitation experiment showing the interaction of hA3G with Smad2/3/4/7 in transfected HEK293T cells. IP, immunoprecipitation; IB, immunoblot. (*B*) Interaction between hA3G and endogenous Smad7 is analyzed by immunoprecipitation assay in HTLV-1-negative T-cell lines (Hut78, H9), an HTLV-1-infected T-cell line (MT-2), and an ATL cell line (ATL55T+). IP, immunoprecipitation; IB, immunoblot. (*C*) GSEA with RNA-seq showing a category of significantly enriched gene signatures related to protein tyrosine kinase activity in hA3G knockdown ATL cells. (*D*) Immunoblot analysis reveals no dose-dependent phosphorylation of Smad2 under expression of hA3G in transfected HepG2 cells. (*E*) Endogenous interaction between HBZ and Smad3 in ATL55T(+) and hA3G-knockdowned ATL55T(+) cells is analyzed by immunoprecipitation assay. IP, immunoprecipitation; IB, immunoblot. The hA3G expression values were analyzed by ImageJ. (*F*) Immunoblot analysis reveals no dose-dependent phosphorylation of Smad2 under expression of HBZ in transfected HepG2 cells. Experiments were performed at least twice (*A-B, D, and F*).

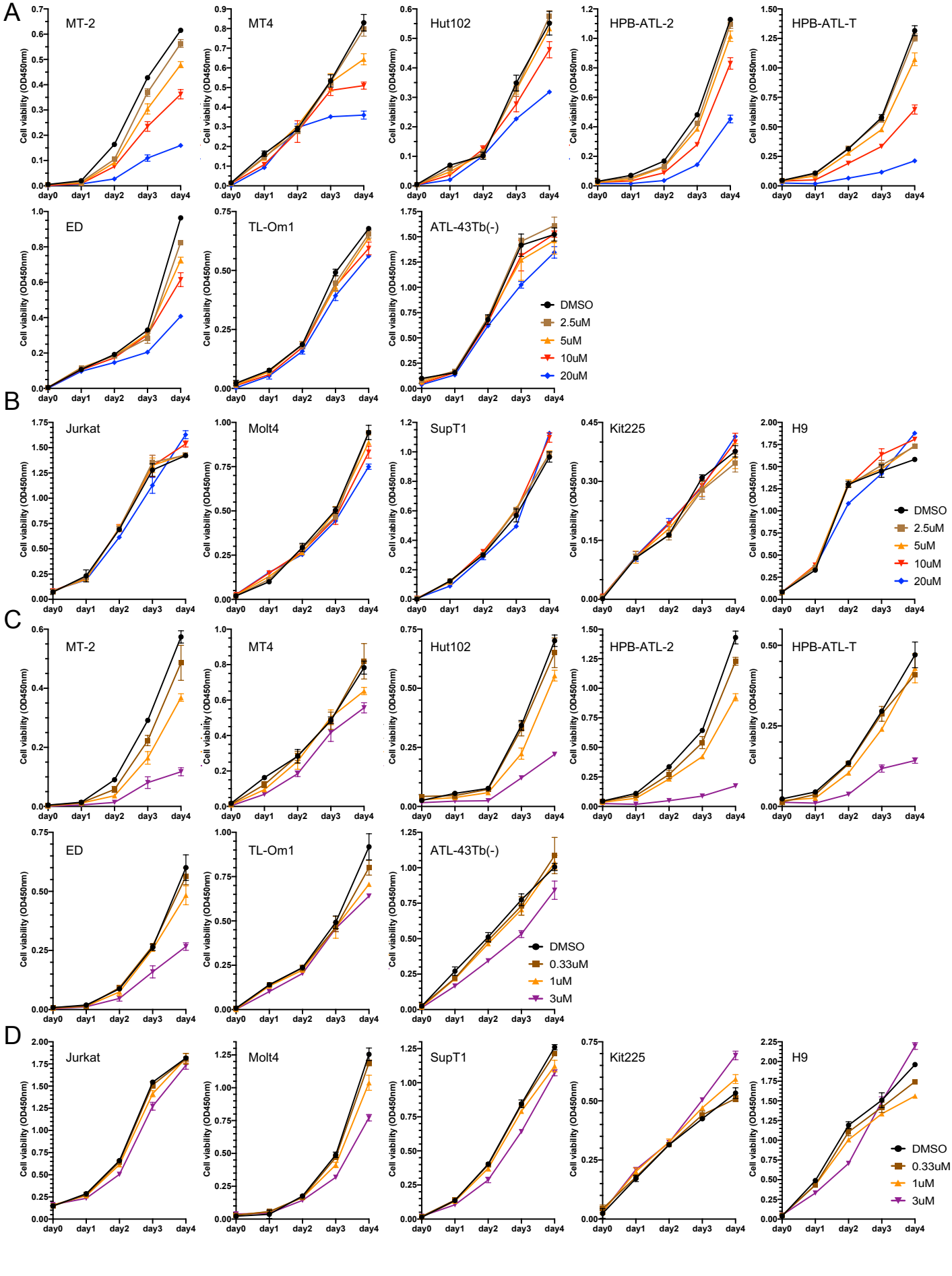
A
MT-2
MT4
Hut102
HPB-ATL-2
HPB-ATL-T
ED
TL-Om1
ATL-43Tb(-)
Cell viability (OD450nm)
day0 day1 day2 day3 day4
DMSO
2.5uM
5uM
10uM
20uM
B
Jurkat
Molt4
SupT1
Kit225
H9
C
0.33uM
1uM
3uM
D

**Fig. S7. Cell growth assays in HTVL-1-non-infected and -infected T-cell lines.**
*(A)* Cell growth of HTLV-1-infected T-cell lines/ATL cell lines treated with SB431542 (normalized mean ± s.d. of triplicate experiments). (*B*) Cell growth of HTLV-1-non-infected T-cell lines treated with SB431542 (normalized mean ± s.d. of triplicate experiments). (*C*) Cell growth of HTLV-1-infected T-cell lines/ATL cells lines treated with SIS3-HCl (normalized mean ± s.d. of triplicate experiments). (*D*) Cell growth of HTLV-1-non-infected T-cell lines treated with SIS3-HCl (normalized mean ± s.d. of triplicate experiments).

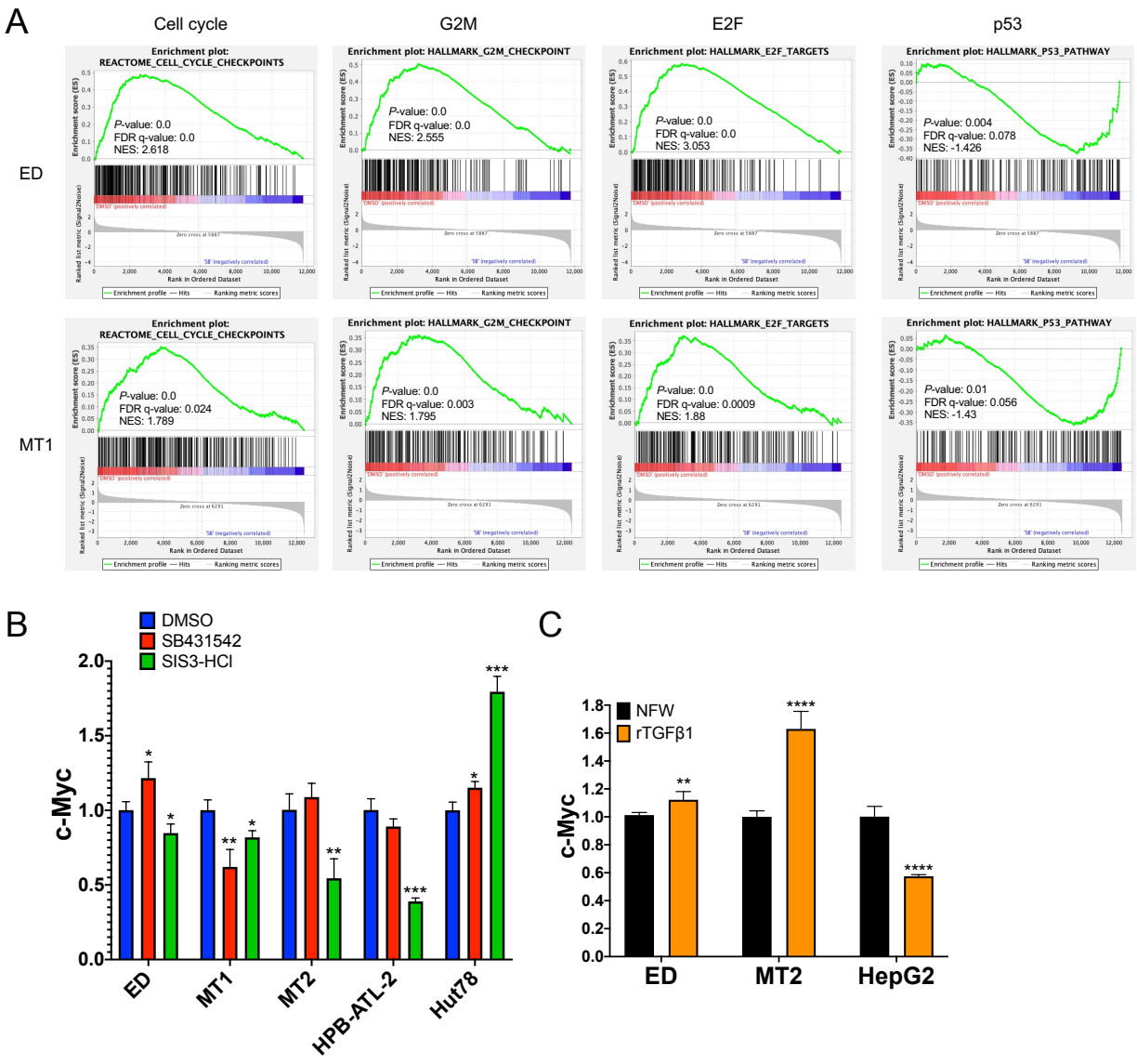


**Fig. S8. MYC is upregulated by the TGF-β/SMAD pathway in HTLV-1-infected cells.** (*A*) Significantly enriched gene signatures for cell cycle related gene sets in ED cells (top) and MT-1 cells (bottom) treated with SB431542, by GSEA with RNA-seq. (*B*) c-*Myc* expression in an HTLV-1-negative T-cell line (Hut78), an HTLV-1-infected T- cell line (MT-2), and ATL cell lines (ED, MT1, HPB-ATL-2) treated with SB431542 or SIS3-HCl, by RT-qPCR (normalized mean ± s.d. of triplicate experiments; one-way ANOVA with Tukey correction; *P < 0.05; **P < 0.01; ***P < 0.001). (*C*) c-*Myc* expression in cell lines treated with or without recombinant TGF-β1 (normalized mean ± s.d. of triplicate experiments; two-tailed unpaired Student's t test; **P < 0.01; **** P < 0.0001). Experiments were performed at least twice (*B*-*C*).

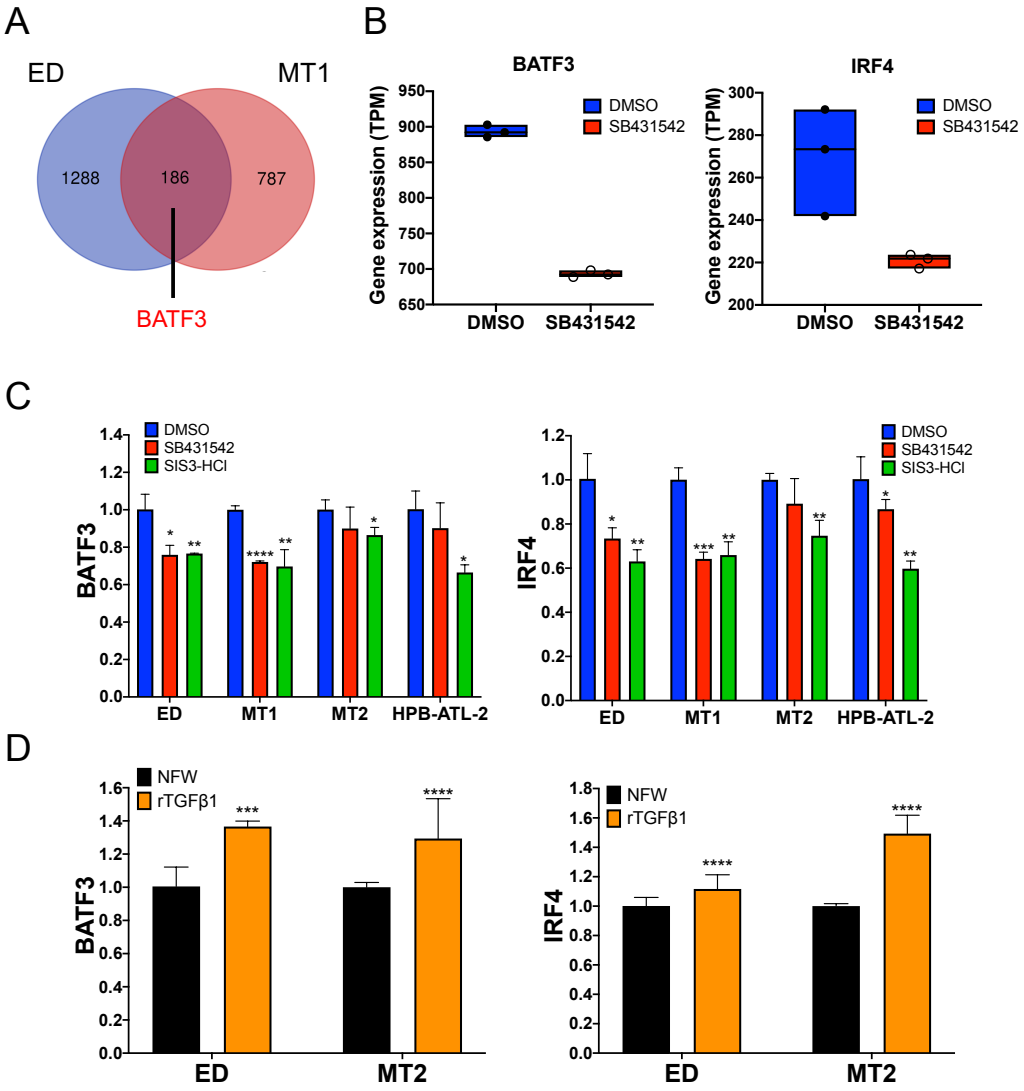


**Fig. S9. BATF3 and IRF4 are upregulated by activation of the TGF-β/SMAD pathway.** **(*A*),** Venn diagram of differentially expressed genes (DEG) by RNA-seq in ED cells and MT-1 cells treated with SB431542. (*B*)**,** Transcripts per million (TPM) of *BATF3* (left) and *IRF4* (right) expression in MT-1 cells treated with SB431542, analyzed by RNA-seq. (*C*)**,** RT-qPCR showing *BATF3* (left) and *IRF4* (right) expression in an HTLV-1-infected T-cell line (MT-2) and ATL cell lines (ED, MT1, HPB-ATL-2) treated with SB431542 or SIS3-HCl (normalized mean ± s.d.; *P < 0.05; **P < 0.01; ***P < 0.001; **** P < 0.0001)**.** **(*D*),** RT-qPCR showing *BATF3* (left) and *IRF4* (right) expression in ED cells and MT-2 cells treated with or without recombinant TGF-β1 (normalized mean ± s.d. of triplicate experiments; two-tailed unpaired Student's t test; ***P < 0.001; **** P < 0.0001). Experiments were performed at least twice (*C-D*).

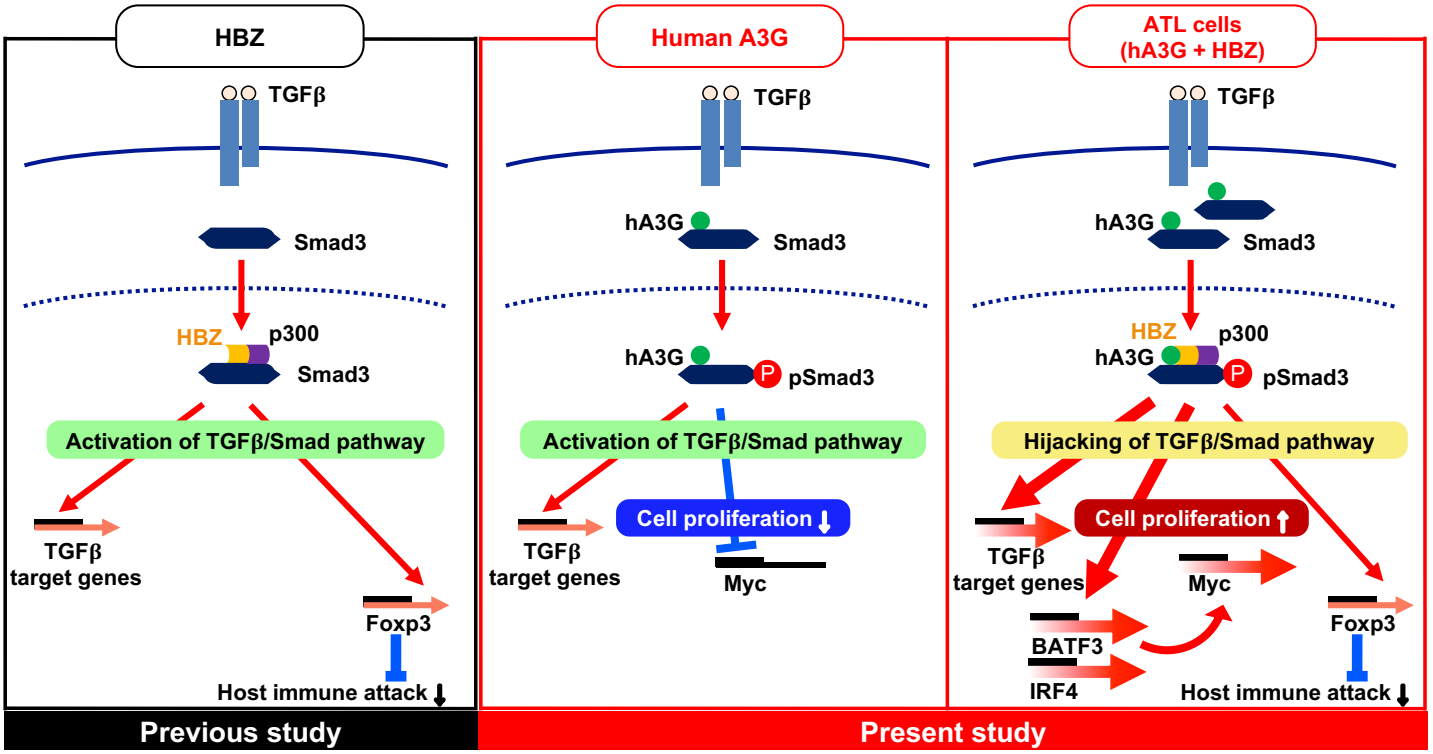


**Fig. S10. Schema of HBZ/hA3G-induced ATL cell proliferation.**
In ATL cells, HBZ and hA3G potentiate the TGF-β/Smad signaling. Enhanced TGF- β/Smad signaling through HBZ/hA3G promotes the proliferation of ATL cells by upregulation of *BATF3/IRF4* and *MYC*.

**Fig. S10**

Table S1. Proviral loads in HTLV-1 asymptomatic carriers, HTLV-2-infected individuals, and STLV-1-infected Japanese macaques

| Cases | PVL (%) | Cases | PVL (%) | Cases | PVL (%) |
|---|---|---|---|---|---|
| HTLV-1 AC1 | 5.4 | HTLV-1 AC34 | 0.5 | HTLV-2#3 | 25.7 |
| HTLV-1 AC2 | 8.2 | HTLV-1 AC35 | 0.2 | HTLV-2#10 | 0.24 |
| HTLV-1 AC3 | 0.5 | HTLV-1 AC36 | 6.8 | HTLV-2#5 | 0.009 |
| HTLV-1 AC4 | 0.1 | HTLV-1 AC37 | 0.8 | HTLV-2#6 | 1.545 |
| HTLV-1 AC5 | 24.9 | HTLV-1 AC38 | 0.03 | HTLV-2#7 | 0.867 |
| HTLV-1 AC6 | 1.2 | HTLV-1 AC39 | 8.0 | HTLV-2#8 | 8.927 |
| HTLV-1 AC7 | 2.5 | HTLV-1 AC40 | 12.5 | HTLV-2#9 | 16.38 |
| HTLV-1 AC8 | 20.0 | HTLV-1 AC41 | 0.4 | HTLV-2#1791 | NA |
| HTLV-1 AC9 | 10.5 | HTLV-1 AC42 | 1.3 | HTLV-2#2204 | NA |
| HTLV-1 AC10 | 4.5 | HTLV-1 AC43 | 5.3 | HTLV-2#1622 | NA |
| HTLV-1 AC11 | 9.3 | HTLV-1 AC44 | 0.9 | HTLV-2#1890 | NA |
| HTLV-1 AC12 | 6.1 | HTLV-1 AC45 | 12.4 | HTLV-2#1875 | NA |
| HTLV-1 AC13 | 3.8 | HTLV-1 AC46 | 3.1 | HTLV-2#1009 | NA |
| HTLV-1 AC14 | 4.6 | HTLV-1 AC47 | 1.5 | HTLV-2#991 | NA |
| HTLV-1 AC15 | 1.5 | HTLV-1 AC48 | 0.2 | HTLV-2#1975 | NA |
| HTLV-1 AC16 | 91.3 | HTLV-1 AC49 | 5.5 | HTLV-2#1073 | NA |
| HTLV-1 AC17 | 4.2 | HTLV-1 AC50 | 3.8 | HTLV-2#416 | NA |
| HTLV-1 AC18 | 1.2 | HTLV-1 AC51 | 2.5 | STLV1-1 | 1.3 |
| HTLV-1 AC19 | 10.0 | HTLV-1 AC52 | 3.2 | STLV1-2 | 1.5 |
| HTLV-1 AC20 | 14.1 | HTLV-1 AC53 | 3.5 | STLV1-3 | 5.9 |
| HTLV-1 AC21 | 1.9 | HTLV-1 AC54 | 7.3 | STLV1-4 | 6.5 |
| HTLV-1 AC22 | 0.2 | HTLV-1 AC55 | 2.2 | STLV1-5 | 9.8 |
| HTLV-1 AC23 | 11.0 | HTLV-1 AC56 | 2.4 | STLV1-6 | 11.5 |
| HTLV-1 AC24 | 1.3 | HTLV-1 AC57 | 1.5 | STLV1-7 | 11.6 |
| HTLV-1 AC25 | 22.6 | HTLV-1 AC58 | 0.3 | STLV1-8 | 13.7 |
| HTLV-1 AC26 | 7.7 | HTLV-1 AC59 | 3.1 | STLV1-9 | 14.1 |
| HTLV-1 AC27 | 3.5 | HTLV-1 AC60 | 1.2 | STLV1-10 | 17.1 |
| HTLV-1 AC28 | 1.9 | HTLV-1 AC61 | 17.7 | STLV1-11 | 53.2 |
| HTLV-1 AC29 | 2.1 | HTLV-1 AC62 | 0.6 | STLV1-12 | 0.2 |
| HTLV-1 AC30 | 10.4 | HTLV-1 AC63 | 3.5 | STLV1-13 | 0.4 |
| HTLV-1 AC31 | 1.3 | HTLV-1 AC64 | 7.8 | STLV1-14 | 1.2 |
| HTLV-1 AC32 | 6.1 | HTLV-1 AC65 | 15.8 | STLV1-15 | 3.3 |
| HTLV-1 AC33 | 0.1 | HTLV-2#1 | 6.0 | STLV1-16 | 0.3 |

Abbreviation: HTLV-1, human T-cell leukemia virus type 1; HTLV-2, human T-cell leukemia virus type 2; STLV-1, simian T-cell leukemia virus type 1; AC, asymptomatic carrier; PLV, proviral load; NA, not available.

Table S2. Primers for quantitative RT-PCR and deep-sequencing analysis

| Gene/target | | Sequence |
|---|---|---|
| Human APOBEC3G | F | 5'-CCGAGGACCCGAAGGTTAC-3' |
| | probe | 5' FAM-ccaggagg-TAMRA 3' |
| | R | 5'-TCCAACAGTGCTGAAATTCG-3' |
| SMAD2 | F | 5'-CTCAAGGCAATTGAAAACTGCG-3' |
| | R | 5'-GGCGGAAGTTCTGTTAGG-3' |
| SMAD3 | F | 5'-GTGACCACCAGATGAACCAC-3' |
| | R | 5'-GTAGTAGGAGATGGAGCACC-3' |
| SMAD7 | F | 5'-CTGTGCCTTCCTCCGCTG-3' |
| | R | 5'-CACTCTCGTCTTCTCCTC-3' |
| BATF3 | F | 5'-CGGAAGAAGCAGACCCAGAA-3' |
| | R | 5'-CATCTTCTCGTGCTCCTTCAGT-3' |
| IRF4 | F | 5'-GACTTTGAGGAACTGGTTGAGC-3' |
| | R | 5'-GTAAGGCGTTGTCATGGTGTAG-3' |
| MYC | F | 5'-CCTGGTGCTCCATGAGGAGAC-3' |
| | R | 5'-CAGACTCTGACCTTTTGCCAGG-3' |
| HBZ | F | 5'-CGACCTGAGCTTTAAACTTACC-3' |
| | R | 5'-GCCCGTCCACCAATTCCTCC-3' |
| HTLV-1 provirus | F | 5'-TACGTCTTTGTTTCGTTTTCTGTTCTGCGCCG-3' |
| | R | 5'-AGAGCCGGCTGAGTCTAGGTAGGCT-3' |
| HTLV-2a provirus | F | 5'-CTCGGCTAGACTCTGCCTTAAACT-3' |
| | R | 5'-TCGACCTGAGAGGAGACTTACCTT-3' |
| HTLV-2b provirus | F | 5'-GTTCTTTCCTCTTCGTCGTCAC-3' |
| | R | 5'-GTGACGACGAAGAGGAAAGAAC-3' |
| STLV-1 provirus | F | 5'-CCGCTGCAGATCGAAAGTTCC-3' |
| | R | 5'-AGAGCCGGCCGAATCTAGG-3' |
| pX1MT-M pX region | F | 5'-GGCCTTACAAACTGGAATCACC-3' |
| | R | 5'-AGAGCCGGCTGAGTCTAGGCAGGCT-3' |
| pH6neo pX region | F | 5'-GAGGATTAGACCTCCTATTCTGGG-3' |
| | R | 5'-CTTCCCCGGGAAGACAATGC-3' |
| pWK1699 pX region | F | 5'-GGCCTTACAAACTGGAATCACC-3' |
| | R | 5'-GAGAGAGTTGTAAAATGGGCTGCT-3' |

Abbreviation: RT-PCR, reverse transcription polymerase chain reaction; F, forward; R, reverse; BATF3, basic leucine zipper ATF-like transcription factor 3; IRF4, interferon regulatory factor 4; HBZ, HTLV-1 bZIP factor.